A coordination π–π framework exhibits spontaneous magnetization†

Lu-Lin Li,[a] Kuan-Jiuh Lin,*[a] Chin-Jun Ho,[b] Chia-Pin Sun[b] and Hung-Duen Yang*[b]

Received (in Cambridge, UK) 4th November 2005, Accepted 17th January 2006
First published as an Advance Article on the web 10th February 2006
DOI: 10.1039/b515681e

A π–π scaffolding framework that was assembled as a one-dimensional chain structure comprising alternating Δ- and Λ-iron(II) chiral building units, $[Fe^{II}(\Delta)Fe^{II}(\Lambda)(ox)_2(phen)_2]_n$, reveals spontaneous magnetization that gives rise to pronounced hysteresis loops below 10 K.

The class of bimetallic oxalato-bridged supramolecular architectures has been intensively studied in the context of molecular-based magnetism.[1–4] These phases can behave as ferro-,[1] ferri-,[2] or antiferro-magnets[3] whose properties depend on the nature of the electronically "innocent" cations and the interactions that may exist within the bimetallic network. In recent years there has been increasing attraction toward the design of two-dimensional architectures constructed from bimetallic oxalato-bridged phases incorporating π-functional organic molecules.[5–7] However, spontaneous magnetization is a rather rare phenomenon in the series of π-functional magnetic materials. Because the presence of π–π interactions may give rise to long-range ferromagnetic ordering between metal ions, a promising approach for creating robust crystals of a coordination π–π framework has been achieved by exploring the efficiency of hydrothermal synthetic technology.[8] In this communication, we report the hydrothermal synthesis of a π-functional sheet-like structure composed of one-dimensional (1D) chains that comprise alternating Δ- and Λ-iron(II) assembled building units, $[Fe^{II}(\Delta)Fe^{II}(\Lambda)(ox)_2(phen)_2]_n$ (**1**). Below 10 K, compound **1** exhibits spontaneous magnetization that gives rise to pronounced hysteresis loops.

We grew deep-red crystals of **1** from a reaction mixture of $FeCl_2{\cdot}4H_2O$, oxalic acid, phen, and water (molar ratio of 2 : 3 : 2 : 4400) that had been heated at 180 °C for 96 h in an autoclave.‡ This hydrothermal synthesis gave **1** in a highly reproducible yield of 62%. We determined the structure of **1** through single-crystal X-ray diffraction (Fig. 1).§ The structure reveals infinite 1D inorganic chains of the type $[-Fe^{II}(\Delta)-C_2O_4-Fe^{II}(\Lambda)-]$ in which the phen ligands are bound to the metal centers. The chain structure of **1** exhibits three intriguing features. First, the backbone of **1** consists of oxalate groups, at which π-functional coplanar groups may serve as adequate superexchange mediators between the bimetallic magnetic orbitals. Second, the incorporated phen groups play an important role in the construction of a π-stacked layer structure between adjacent crystallographically symmetry-related chains, which causes the layered framework and may couple magnetically. The π–π distance of phen groups is only 3.77 Å. Third, the asymmetric unit contains two crystallographically distinct Fe^{II} atoms, each of which is chelated by the four oxygen atoms from two distinct oxalate groups and two nitrogen atoms of the phen groups. Both metal coordination spheres are highly distorted octahedra possessing bond angles that are far from the ideal values of 180° and 90° [*i.e.*, O(2)–Fe(1)–O(6), 163.0(2); O(2)–Fe(1)–N(1), 102.5(3); O(4)–Fe(2)–O(5), 163.5(2); O(4)–Fe(2)–N(4), 100.2(3)], but the Fe–O and Fe–N bond lengths are within the ranges observed in most iron(II) complexes [bond valence sums (BVS): Fe(1) 2.28, Fe(2) 2.23]. A detailed description of the coordination spheres of both iron atoms must take into account the potential for isomerism resulting from octahedral arrangement of the MX_3Y_3 type, which can lead to Δ and Λ enantiomers. Indeed, within a chain, the Fe^{II} ions that possess D_3-like point group symmetry present a perfect alternation of Δ and Λ chiral sites. Moreover, the adjacent layers are stacked on top of each other along the *b* axis and glued by cooperative CH···O interactions (C(21)–H···O(7) 3.482 Å, C(14)–H···O(8) 3.143 Å).

The magnetic susceptibility χ of **1** was measured in the temperature range from 1.8 to 300 K and an applied field of

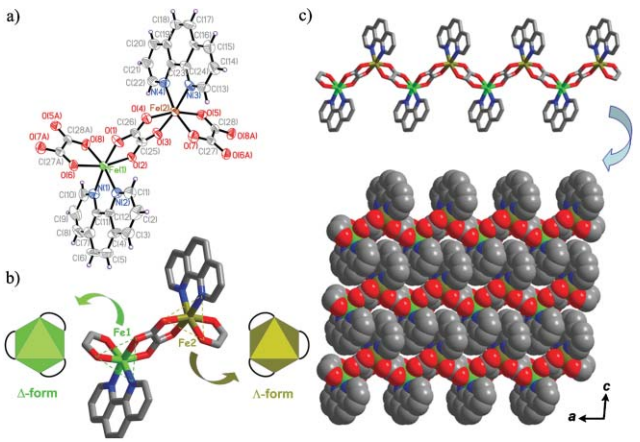

Fig. 1 a) An ORTEP plot of a section of an infinite chain in **1** (50% probability ellipsoid). Selected bond lengths [Å]: Fe(1)–O(2) 2.095(6), Fe(1)–O(6) 2.117(6), Fe(1)–O(8) 2.124(7), Fe(1)–O(1) 2.165(7), Fe(1)–N(1) 2.183(8), Fe(1)–N(2) 2.140(7), Fe(2)–O(4) 2.114(6), Fe(2)–O(5) 2.121(6), Fe(2)–O(7) 2.139(7), Fe(2)–O(3) 2.146(6), Fe(2)–N(3) 2.177(7), Fe(2)–N(4) 2.168(8). b) Schematic illustration of the asymmetric unit of **1**, displaying the two distinct Δ(Fe1) and Λ(Fe2) chiral centers. c) Space-filling view of the *ac* plane displaying the corrugated π–π network constructed from iron–oxalate chains incorporating phen molecules. The π–π distance of 3.77 Å calculated from the centroid of the ring with N(2)–C(1)–C(2)–C(3)–C(4)–C(12) to the C(16)–C(17)–C(18)···C(24) ring at (x,y,1 + z). Green, Fe1; gold, Fe2; red, O; blue, N; gray, C; purple, H.

[a]*Department of Chemistry, Center of Nanoscience and Nanotechnology, National Chung-Hsing University, Taichung 402, Taiwan (Republic of China). E-mail: kjlin@dragon.nchu.edu.tw*
[b]*Department of Physics, Center of Nanoscience and Nanotechnology, National Sun Yat-Sen University, Kausiung 804, Taiwan (Republic of China). E-mail: yang@mail.phys.nsysu.edu.tw*

† Electronic supplementary information (ESI) available: Fig. S1. Temperature dependence of $\chi_m T$ for compound **1**. See DOI: 10.1039/b515681e

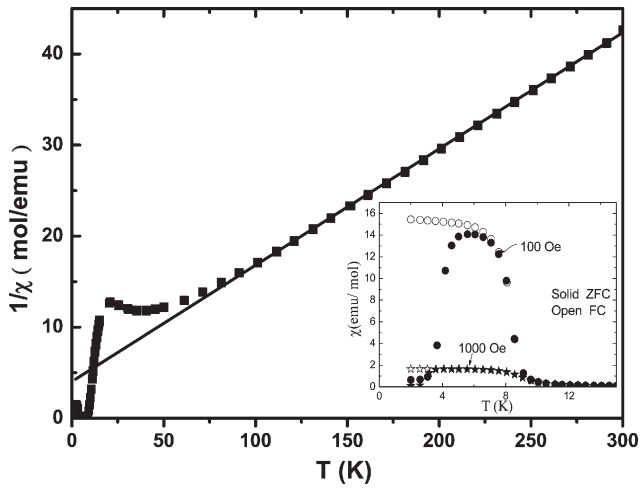

Fig. 2 Temperature dependence of inverse magnetic susceptibility $1/\chi$ of **1**. The inset shows the low temperature zero-field-cooled (ZFC) and field-cooled (FC) magnetic susceptibility at applied magnetic fields of 100 and 1000 Oe.

1000 Oe.¶ The temperature dependence of inverse magnetic susceptibility ($1/\chi$) shown in Fig. 2 follows the paramagnetic Curie–Weiss law, $\chi = C/(T - \theta)$ at temperatures above 100 K. The fitting yields the Curie constant $C = 7.82$ emu K/mol and the Weiss temperature $\theta = -31.6$ K. The effective magnetic moment $\mu_{eff} = 5.59\ \mu_B$ can be calculated from C indicating the high spin state of Fe^{II}. The large and negative Weiss temperature then indicates an antiferromagnetic ordering at low temperature. The onset of long-range magnetic ordering transition can be evidently seen in the inset of Fig. 2, where there is shown a rapid rise below 10 K and a peak in the zero-field-cooled (ZFC) magnetic susceptibility and saturation at the lower temperature in the field-cooled (FC) one. In fact, the rapid suppression of the peak in χ by magnetic field indicates an antiferromagnetic ordering in nature, while the observation of saturation (also suppressed by field) reflects (weak) ferromagnetic-ordering character.

To further confirm the magnetic ordering and to determine its transition temperature T_m, ac susceptibility measurements were performed and the results are shown in Fig. 3. A sharp peak is clearly observed both in in-phase χ' and out of phase χ''. The T_m = 8.6 K thus was determined at the temperature where the χ'' starts to appear. Though the peak position increases and the amplitude decreases slightly with increasing frequency, the T_m remains almost constant. Therefore, a small particle size of sample is expected due to this small variation in frequency.[9] Nevertheless, a clearly seen peak in ac susceptibility somehow indicates that the magnetic ordering is either ferromagnetic or ferrimagnetic or canted antiferromagnetic.

To further explore the nature of magnetic spin structure for this material, the field-dependent isothermal magnetization was, as demonstrated in Fig. 4, measured at temperatures of 2.5, 4 K and 10 K and magnetic field from −5000 Oe to 5000 Oe. Indeed, a profound and quite large hysteresis loop is observed at $T = 2.5$ K ($T < T_m$). A coercive field of 3000 Oe was estimated in this case. Combining these data (Figs. 2–4), two possible magneto-structural mechanisms are suggested to describe the spontaneous magnetization. One is single-chain magnet (SCM)[10] behavior in which antiferromagnetic interactions exist within each chain and produce ferrimagnetic ordering like spin-canted materials. The spin-canted structure should arise from the antisymmetric exchange mechanism,[11] and is consistent with the lack of an inversion center between neighboring Fe^{II} ions within the 1D chain. However, the ferrimagnetic order within the chains may not sufficiently explain the strong ferromagnetic order at low temperature. Another interpretation may be associated with the 2D π-stacked magnetic-coupling that may arise from the charge transfer through phen groups to metal iron centres.[12] We have observed from our X-ray diffraction data that the angle between the metal and the centroid of oxalate planes is 176°; this value, however, will not produce a

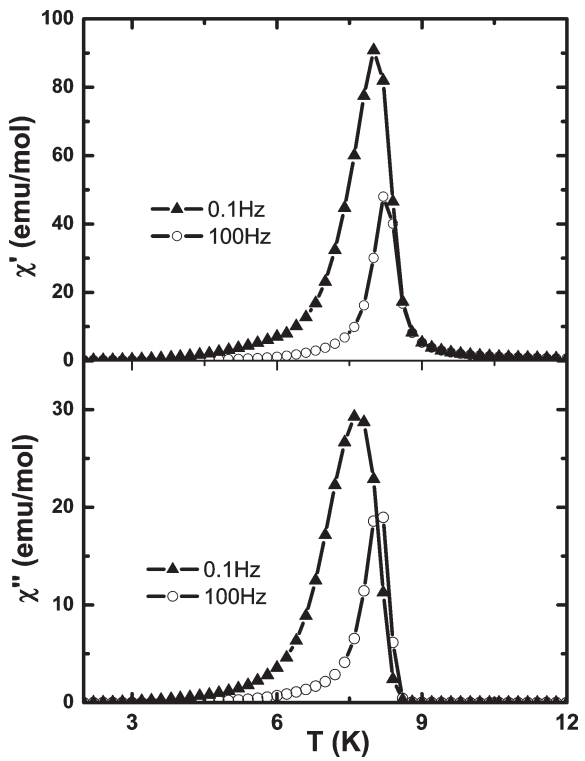

Fig. 3 In phase χ' and out of phase χ'' ac susceptibility under the frequency of 0.1 and 100 Hz.

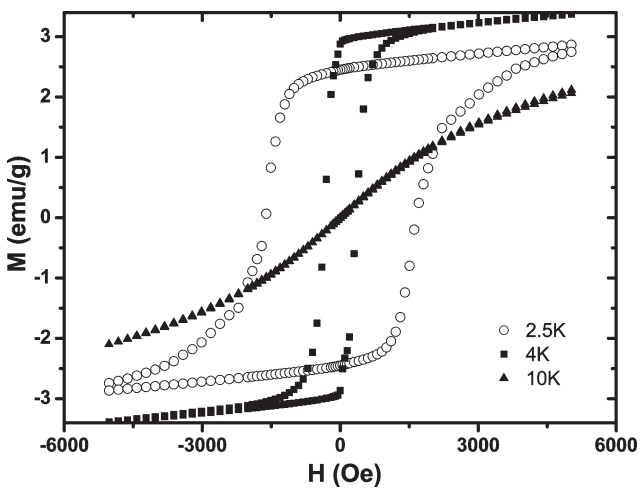

Fig. 4 Hysteresis loops for **1** at 2.5, 4 K and 10 K with sweeping magnetic field from −5000 to +5000 Oe.

small degree of ferromagnetic ordering. The only possible alignment is along the direction from an iron atom toward the center of a phen plane, which has an angle of 169°, which deviates somewhat from the angle of a totally anti-parallel arrangement (180°). Although the spins of neighboring Fe^{II} within each chain are basically antiferromagnetically coupled, they are not totally compensated, because of their slightly different coordination spheres as well as a small difference in certain angles within the 1D structure, leading therefore to 1D 'weak ferromagnetism'.[13] Due to the fact that the next-nearest distance between pairs of Fe^{II} ions is an interchain distance of 7.337 Å, we thus surmise that the ferromagnetic coupling through the π-stacked phen ligands might also contribute to the observed ferromagnetism.

Compound **1** provides the first example of π–π scaffolding that is capable of producing quite strong ferromagnetic order at low temperature though the intrachain coupling is basically antiferromagnetic between alternating chiral Λ- and Δ-iron(II) centers. The observed saturation of magnetization and hysteresis loop below T_m are significantly larger than those of other iron-containing clusters.[14] Further work on thermodynamic measurements regarding the nature of the magnetic ordering transition and neutron scattering experiments for solving the exact spin structure are in progress.

This work was supported by the National Science Council of Taiwan (NSC-94-2113-M005-004; NSC-94-2120-M007-002; NSC-94-2112-M110-014).

Notes and references

‡ Synthesis of **1**: A reaction mixture of $FeCl_2{\cdot}4H_2O$ (0.0398 g, 0.2 mmol), oxalic acid (0.0378 g, 0.3 mmol), 1,10-phenanthroline monohydrate (0.0396 g, 0.2 mmol), H_2O (8 mL, 440 mol) in molar ratios of 2 : 3 : 2 : 4400 and 0.2 mL CsOH was sealed in a 23 mL Teflon-lined stainless-steel autoclave, heated to 100 °C within 2 h at a rate of 120 °C h^{-1}, heated at 180 °C for 96 h, cooled to 70 °C at a rate of 6 °C h^{-1}, and then left to cool to room temperature. The resulting deep-red fan-shaped crystals were collected by filtration, washed with EtOH, and dried in air. The yield of **1** (62%) was based on $FeCl_2$. This synthesis was reproducible. Complex **1** is insoluble in CH_3CN, CH_2Cl_2, EtOH, and H_2O. Elemental analysis: calcd. C 51.89, H 2.49, N 8.64; found C 51.21, H 3.06, N 8.30%. Thermogravimetric analysis (TGA) reveals that **1** is thermally stable at temperatures up to 310 °C; *i.e.*, no weight loss was observed below 310 °C.

§ Crystal data for **1**: $C_{28}H_{16}Fe_2N_4O_8$, Mr = 648.15, crystal size: 0.2 × 0.125 × 0.1 mm; monoclinic; space group $P2_1$; a = 9.2288(8), b = 13.578(1), c = 10.2001(9) Å; β = 94.310(2)°; V = 1274.5(2) $Å^3$; Z = 2; σ = 1.689 Mg m^{-3}; $2\theta_{max}$ = 55°; 8155 reflections measured, 5235 unique (R_{int} = 0.065) which were used in all calculations. R_1 = 0.063, $wR_2(F^2)$ = 0.127, and GOF = 0.964. Flack's parameter = 0.05(4). CCDC 256613. For crystallographic data in CIF or other electronic format see DOI: 10.1039/b515681e

¶ Magnetic susceptibility measurements were performed on crystalline samples using a superconducting quantum interference device (SQUID) magnetometer (Commercial Quantum Design MPMS-XL-6). DC data were measured in the range 1.8–300 K with an applied static field of 1000 Oe. Zero-field-cooled (ZFC) susceptibility means that the sample is first cooled to the lowest temperature (1.8 K) without field, then field is applied and data taken as the temperature is raised; subsequently taking data as the temperature is lowered is called field-cooled (FC). AC data were measured in the range 1.8–12 K with an applied alternating field of 3.95 Oe. The hysteresis loop was obtained upon sweeping the magnetic field between −5000 Oe and +5000 Oe at 2.5, 4 and 10 K.

1 E. Coronado, J. R. Galan-Mascaros, C. J. Gomez-Garcia and V. Laukhin, *Nature*, 2000, **408**, 447–449.
2 C. Mathonière, C. J. Nuttall, S. G. Carling and P. Day, *Inorg. Chem.*, 1996, **35**, 1201–1206.
3 S. Decurtins, H. W. Schmalle, R. Pellaux, R. Huber, P. Fischer and B. Ouladdiaf, *Adv. Mater.*, 1996, **8**, 647–651.
4 H. Tamaki, Z. J. Zhong, N. Matsumoto, S. Kida, M. Koikawa, N. Achiwa, Y. Hashimoto and H. Okawa, *J. Am. Chem. Soc.*, 1992, **114**, 6974–6979.
5 G. Marinescu, M. Andruh, M. Julve, F. Lloret, R. Llusar, S. Uriel and J. Vaissermann, *Cryst. Growth Des.*, 2005, **5**, 261–267.
6 J. Y. Lu, T. J. Schroeder, A. M. Babb and M. Olmstead, *Polyhedron*, 2001, **20**, 2445–2449.
7 G. Marinescu, D. Visinescu, A. Cucos, M. Andruh, Y. Journaux, V. Kravtsov, Y. A. Simonov and J. Lipkowski, *Eur. J. Inorg. Chem.*, 2004, 2914–2922.
8 L. W. Huang, C. J. Yang and K. J. Lin, *Chem. Eur. J.*, 2002, **8**, 396–400.
9 E. Coronado, J. R. Galan-Mascaros, C. J. Gomez-Garcia and J. M. Martinez-Agudo, *Inorg. Chem.*, 2001, **40**, 113–120.
10 H. Miyasaka, T. Nezu, K. Sugimoto, K. Sugiura, M. Yamashita and R. Clerac, *Chem. Eur. J.*, 2005, **11**, 1592–1602.
11 S. J. Rettig, A. Storr, D. A. Summers, R. C. Thompson and J. Trotter, *J. Am. Chem. Soc.*, 1997, **119**, 8675–8680.
12 T. Glaser, M. Heidemeier, S. Grimme and E. Bill, *Inorg. Chem.*, 2004, **43**, 5192–5194.
13 E.-Q. Gao, S.-Q. Bai, Z.-M. Wang and C.-H. Yan, *J. Am. Chem. Soc.*, 2003, **125**, 4984–4985.
14 D. Gatteschi, A. Caneschi, L. Pardi and R. Sessoli, *Science*, 1994, **265**, 1054–1058.

